https://doi.org/10.5194/acp-2021-493
Preprint. Discussion started: 6 July 2021

Atmospheric Chemistry and Physics Discussions

Mercury isotopic compositions in fine particles and offshore surface seawater in a coastal area of East China: Implication for Hg sources and atmospheric transformations

Lingling Xu[a,b,*], Jiayan Shi[b,d], Yuping Chen[a,b,c], Yanru Zhang[a,b,c], Mengrong Yang[a,b], Yanting Chen[a,b], Liqian Yin[a,b], Lei Tong[a,b], Hang Xiao[a,b], Jinsheng Chen[a,b,*]

[a] *Center for Excellence in Regional Atmospheric Environment, Institute of Urban Environment, Chinese Academy of Sciences, Xiamen 361021, China*

[b] *Key Lab of Urban Environment and Health, Institute of Urban Environment, Chinese Academy of Sciences, Xiamen 361021, China*

[c] *University of Chinese Academy Sciences, Beijing 100049, China*

[d] *College of Resources and Environment, Fujian Agriculture and Forestry University, Fuzhou 350002, China*

* Corresponding author.

E-mail address: jschen@iue.ac.cn (J.S. Chen); linglingxu@iue.ac.cn (L.L. Xu)

https://doi.org/10.5194/acp-2021-493
Preprint. Discussion started: 6 July 2021


Atmospheric Chemistry and Physics Discussions

Abstract. Isotopic compositions of Hg in atmospheric particles (Hg_{PM}) are probably the mixed results of emission sources and atmospheric processes. Here, we present Hg isotopic compositions in daily fine particles ($PM_{2.5}$) collected from an industrial site (CX) and a nearby mountain site (DMS) in a coastal area of East China, as well as in surface seawater close to the industrial area, to reveal the roles of anthropogenic emission sources and atmospheric transformations in varying Hg isotopes. The $PM_{2.5}$ samples displayed significant spatial difference in $\delta^{202}Hg$. For the CX, the negative $\delta^{202}Hg$ values were similar to those of source materials and Hg_{PM} contents were well correlated with other chemical tracers, indicating the dominant contributions of local industrial activities to $Hg_{PM2.5}$. Whereas the observed positive $\delta^{202}Hg$ at the DMS was likely associated with regional emissions and extended photo-reduction during transport. $\Delta^{199}Hg$ values in $PM_{2.5}$ from the CX and DMS were comparable positive. The unity slope of $\Delta^{199}Hg$ versus $\Delta^{201}Hg$ over all data suggests that the odd-MIF of $Hg_{PM2.5}$ was primarily induced by photo-reduction in aerosols. The positive $\Delta^{200}Hg$ values with minor spatial difference were probably associated with photo-oxidation of Hg^0 which is generally enhanced in the coastal environment. Total Hg in offshore surface seawater was characterized by negative $\delta^{202}Hg$ and near-zero $\Delta^{199}Hg$ and $\Delta^{200}Hg$, which are indistinguishable from Hg isotopes of source materials. Overall, industrial $PM_{2.5}$ had comparable $\delta^{202}Hg$ values but more positive $\Delta^{199}Hg$ and $\Delta^{200}Hg$ as compared to surface seawater. The results indicate that atmospheric transformations would induce significant fractionation of Hg isotopes, which obscures Hg isotopes of anthropogenic emissions.

Keywords: Particle bound mercury; Surface seawater; Hg isotopes; Mercury sources; Photo-chemical processes.

https://doi.org/10.5194/acp-2021-493
Preprint. Discussion started: 6 July 2021


Atmospheric Chemistry and Physics Discussions

1. Introduction

Mercury (Hg) is a genotoxic element and was ranked with the priority controlled pollutants in many countries. Atmospheric Hg was operationally defined as three forms: gaseous elemental mercury (GEM), gaseous oxidized mercury (GOM), and particle bound mercury (PBM or Hg_{PM}) (Schroeder and Munthe, 1998). Previous studies indicated that Hg_{PM} concentrations in urban and industrial areas could reach up to hundreds even thousands of pg m^{-3}, relative to tens of pg m^{-3} in uncontaminated remote areas (Fu et al., 2015; Mao et al., 2016). Hence, particulate matter (PM) can act as a vector of toxic Hg and inhalation of Hg-carrying particles is an important pathway of human exposure to atmospheric Hg. Atmospheric Hg_{PM} can be directly derived from human activities and scavenged by deposition. In China, coal combustion, non-ferrous metal smelting, and cement production were considered as the three primary emission sources of atmospheric Hg (Zhang et al., 2015). On the other hand, Hg_{PM} undergoes complex transformation processes in the atmosphere. Hg_{PM} can be formed by the uptake of GOM in particles, which made an important contribution to Hg_{PM} in heavily particle polluted areas (Xu et al., 2020). Whereas the reduction of GOM binding with dissolved organic carbon ligands in aqueous particles potentially converts it back to gas phase (Horowitz et al., 2017). The research have suggested that atmospheric Hg_{PM} is generally a combined result of anthropogenic emissions and atmospheric transformations.

Analysis technique of Hg isotopes and mechanisms of Hg isotopic fractionation have come a long way in the last decade (Blum and Johnson, 2017). Hg has seven stable isotopes (including ^{196}Hg, ^{198}Hg, ^{199}Hg, ^{200}Hg, ^{201}Hg, ^{202}Hg, and ^{204}Hg) and exhibits mass dependent fractionation (MDF) and mass independent fractionation (MIF) in various environmental samples and processes (Sonke and Blum, 2013; Yin et al., 2014a; Blum and Johnson, 2017). MDF of Hg isotopes is often reported as $\delta^{202}Hg$, while MIF of odd mass-numbered Hg isotopes (odd-MIF) is reported as $\Delta^{199}Hg$ and $\Delta^{201}Hg$ and MIF of even Hg isotopes (even-MIF) as $\Delta^{200}Hg$ and $\Delta^{204}Hg$. Previous laboratory and field studies have revealed that nearly all biogeochemical processes induce MDF of Hg isotopes, whereas significant odd-MIF of Hg occurs mainly in

https://doi.org/10.5194/acp-2021-493
Preprint. Discussion started: 6 July 2021


Atmospheric Chemistry and Physics Discussions

photochemical processes (Bergquist and Blum, 2007; Malinovsky et al., 2010; Blum et al., 2014; Sun et al., 2016a). What's more, specific ratios of $\Delta^{199}Hg/\Delta^{201}Hg$ have been reported for different transformation processes, i.e., ~1.0 for photo-reduction and ~1.6 for photo-oxidation (Bergquist and Blum, 2007; Sun et al., 2016a). Even-MIF of Hg isotopes is observed mostly in atmosphere related samples, which is suggested to associate with photo-oxidation of Hg^0 by UV and oxidants (Chen et al., 2012; Blum and Johnson, 2017; Fu et al., 2019). Therefore, Hg isotopes are capable of becoming useful tracers for biogeochemical cycles of Hg in the environment.

Little literature is available on Hg isotopes of atmospheric samples due to the difficulty in sampling enough Hg mass for isotopes analysis. Even so, Hg isotopic compositions of atmosphere related samples, like speciated Hg, precipitation, and lichen, have been reported in recent years (Carignan et al., 2009; Gratz et al., 2010; Sherman et al., 2010; Chen et al., 2012; Rolison et al., 2013; Demers et al., 2013, 2015; Fu et al., 2016, 2018, 2019; Yu et al., 2016, 2020). Many studies have measured Hg isotopes in PM to investigate its potential sources and transformation processes in the atmosphere. In general, Hg_{PM} in urban areas which is mainly impacted by local anthropogenic sources has negative MDF and near-zero odd-MIF (Rolison et al., 2013; Das et al., 2016; Huang et al., 2016, 2019, 2020; Huang et al., 2018; Xu et al., 2019). While Hg_{PM} in remote and coastal areas displays more significant odd-MIF, likely linking to enhanced photo-reactions (Rolison et al., 2013; Fu et al., 2019). To date, the fractionation of Hg isotopes in atmospheric processes has not been well elucidated, which hampers application of Hg isotopes in tracking the transfer and transformation paths of Hg.

This study determined Hg isotopic compositions in $PM_{2.5}$ collected from an industrial site and a mountain site in a coastal area of East China. Comparison of $Hg_{PM2.5}$ isotopes at the two neighbouring sites would eliminate the impacts of meteorology and atmospheric Hg background which vary across space on Hg_{PM} isotopes. Furthermore, this study measured isotopic compositions of total mercury (THg) in surface seawater close to the industrial area and distinguished Hg isotopes between atmospheric sample and surface media. The objective of this study is to

https://doi.org/10.5194/acp-2021-493
Preprint. Discussion started: 6 July 2021


Atmospheric Chemistry and Physics Discussions

120 reveal the roles of anthropogenic sources and atmospheric transformations in varying
121 Hg_{PM} isotopic compositions.

122 **2. Experiment**

123 *2.1. Study area description*

124 $PM_{2.5}$ sampling was conducted at an industrial site (Chunxiao, CX) and a nearby
125 mountain site (Daimeishan, DMS) on the east coast of Zhejiang province, East China
126 (Fig. 1). The study region experiences a typical subtropical monsoon climate, with sea
127 breeze in summer and continental breeze in winter. The average annual temperature,
128 precipitation, relative humidity, and sunshine hours were 18.1 ℃, 1608 mm, 76.8%,
129 and 1797 h, respectively.

130 The CX (121.91° E, 29.87° N, 15 m a.g.l.) is located in the Urban Environment
131 Observation and Research Station, Chinese Academy of Sciences, Beilun District,
132 Ningbo. Ningbo is a highly industrial city and there are a high density of industrial
133 activities around the CX. Potential Hg point sources include a large coal-fired power
134 plant (5000 MW) approximately 20 km to the northwest, a Chlor-alkali plant 20 km to
135 the northeast, and an automobile assembly plant within 1 km of the site. The CX is in
136 close proximity to the East China Sea (ECS, ~ 0.6 km), thus clean air masses from the
137 sea in warm seasons would dilute atmospheric Hg at the CX. The concentration of
138 GEM at the CX was reported to be 2.44 ng m^{-3} from Dec. 2016 to Nov. 2017 in a
139 previous study (Yi et al., 2020).

140 The DMS (121.62° E, 29.68° N, 450 m a.s.l.) is located at the summit of
141 Mountain Damei, which is surrounded by trees. The site is 20 km to the coast of the
142 ECS and approximately 22 km south of Ningbo. There are no significant Hg point
143 sources within a radius of ~10 km from the DMS. However, an early study reported
144 that intense regional emissions and long-range transport of Hg usually caused a high
145 atmospheric Hg concentration at the DMS (mean: 3.3 ng m^{-3}, from Apr. 2011 to Apr.
146 2013; Yu et al., 2015).

147 Surface seawater samples were collected in the offshore area of Ningbo. The
148 seawater sampling area (about 122.04° E, 29.82° N, Fig. 1) is approximately 1 km
149 west of the Beilun District, Ningbo.

https://doi.org/10.5194/acp-2021-493
Preprint. Discussion started: 6 July 2021

Atmospheric Chemistry and Physics Discussions

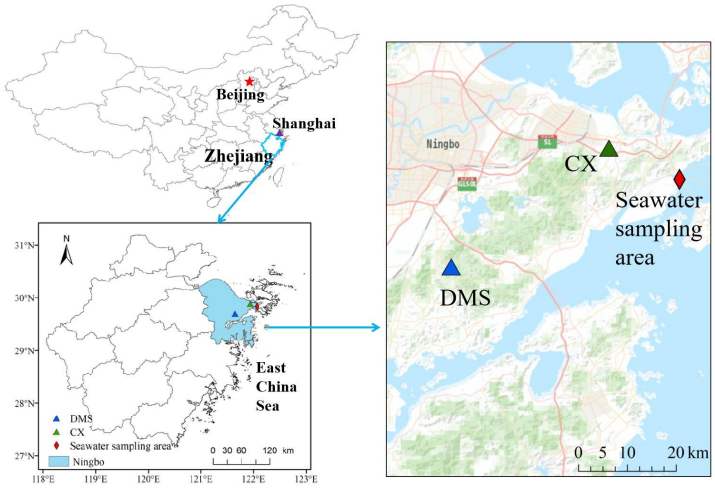

Fig. 1 Locations of $PM_{2.5}$ (CX: industrial site; DMS: mountain site) and surface seawater sampling area.

2.2. Sample collection and analysis

2.2.1. Sampling of $PM_{2.5}$

The period of $PM_{2.5}$ sampling was from Jul. 2017 to Jun. 2018. Daily $PM_{2.5}$ samples were collected 1~2 times a week at the CX (except Jan. and Feb. 2018) and once a week at the DMS. Field blank sample was collected at each site. $PM_{2.5}$ samples were collected on preheated quartz-fiber filter (500 ℃, 4 h, 8 × 10 inch, Whatman) using a high volume sampler (Tianhong TH1000H, China) with a flow rate of 1.05 m^3 min^{-1}. The filters were conditioned at 24 ± 1 ℃ and 52 ± 2%. The mass loading of $PM_{2.5}$ on filters was determined by mass difference before and after sampling. A total of 64 and 36 filter samples were collected at the CX and DMS, respectively. The filter samples were wrapped in aluminum foils and stored at -20 ℃ until analysis.

2.2.2. Concentration of Hg and other chemical species in $PM_{2.5}$

Six punches (ca. 0.5 cm^2 per punch) of each sampling filter were digested by a 10 mL of 40% aqua regia (HNO_3: HCl = 1:3, *v/v*) in a water bath at 95 ℃ for 5 min, then the solution was oxidized by 1 mL BrCl and bathed for another 30 min. After cooling down, the extracted solution was diluted to 15 mL with ultra-pure water and then analyzed by cold-vapor atomic fluorescence spectrometry (CVAFS, Brooks Rand Model III, USA) following the EPA method 1631. The content of Hg on blank filters

https://doi.org/10.5194/acp-2021-493
Preprint. Discussion started: 6 July 2021


Atmospheric Chemistry and Physics Discussions

171 can be negligible (42.5 pg at the CX and 27.0 pg at the DMS) relative to those on
172 sample filters.

173 Selected $PM_{2.5}$ samples analyzed for Hg isotopes were also measured for 8 water
174 soluble inorganic ions (K^+, Ca^{2+}, Na^+, Mg^{2+}, Cl^-, SO_4^{2-}, NO_3^-, and NH_4^+), elemental
175 carbon (EC), organic carbon (OC), and levoglucosan. The water soluble ions were
176 analyzed by an ion chromatography (ICS-3000, Dionex, USA). EC and OC were
177 analyzed using a carbon analyzer (Model 4, Sunset Lab., USA) and NOISH protocol.
178 Analytical procedures and quality control procedures have been described by Xu et al.
179 (2018). Levoglucosan, an excellent indicator of biomass burning, was analyzed using
180 a gas chromatography – mass spectrometer detector (GC – MS, Agilent 7890A-5975C,
181 Agilent Tech. Inc., USA). Levoglucosan analytical procedures have been presented in
182 detail elsewhere (Hong et al., 2019).

183 *2.2.3. Sampling and analysis of Hg in seawater*

184 Seawater samples were collected from the surface of offshore sampling area
185 twice a month during Jul. 2017 ~ Jun. 2018, except Feb. 2018. Each time, three
186 duplicate seawater samples were collected for THg content analysis. Final THg
187 content was determined by the average of three duplicate samples. In addition, ~2 L
188 surface seawater was sampled for Hg isotopes analysis each time. The seawater
189 samples were stored in brown glass bottles and preserved with 1% (*v/v*) HCl in the
190 laboratory. They were analyzed for Hg content and isotopic compositions in a month.

191 Total Hg content in seawater samples was measured by the CVAFS (Brooks
192 Rand Model III, USA). A 25 mL of seawater sample was digested with 0.2 M BrCl at
193 least 12 h in advance and then analyzed using the EPA method 1631. More details can
194 be found in a previous study (Xu et al., 2014). Method blank was processed by bottles
195 filling up with ultra-pure water instead of seawater. The blank was lower than 10 pg
196 (n = 15), which can be negligible compared to the samples.

197 *2.3. Analysis of Hg isotopic compositions*

198 *2.3.1. $PM_{2.5}$ sample processing*

199 Due to effects of precipitation and short sampling duration, the mass of Hg on
200 most of $PM_{2.5}$ samples was not sufficient for isotopes detection. A total of 10 $PM_{2.5}$

https://doi.org/10.5194/acp-2021-493
Preprint. Discussion started: 6 July 2021


Atmospheric Chemistry and Physics Discussions

samples from each site were analyzed for Hg isotopes. Pre-concentration of Hg from $PM_{2.5}$ samples was conducted following a dual-stage combustion protocol (Huang et al., 2015). To be specific, a tube furnace (OTF-1200X-II, Kejin, China) consisting of two combustion stages was used. A sampling filter was embedded in a furnace quartz tube (50 mm OD, 46 mm ID, 80 cm length). The tube was then placed in the furnace so that the filter was at the first combustion stage. The second decomposition stage was heated up in advance and maintained at 1000 °C, then the first combustion stage was heated up to 950 °C through a temperature-programmed procedure. The released Hg was transferred by O_2/Ar gas (30%/70%) at a flow rate of 20 mL min^{-1} and then trapped by a 10 mL of 40% inverse aqua regia.

2.3.2. Seawater sample processing

A total of 20 seawater samples were analyzed for Hg isotopes. ~2 L seawater sample was mixed with a $NH_2OH{\cdot}HCl$ solution for neutralizing excess BrCl and then a $SnCl_2$ solution for reducing the oxidized Hg. The pre-treated seawater sample was stirred and bubbled for 1 h with Hg-free N_2 at a flow rate of 400 mL min^{-1}. The gaseous Hg purged off seawater samples was collected by a series of three gold traps. The gold traps were heated and the released Hg was transferred by Hg-free N_2 at 10~15 mL min^{-1} and concentrated by a 10 mL of 40% inverse aqua regia.

2.3.3. Hg isotopes analysis

All trapping solutions were preserved with 1% (*v/v*) BrCl and stored at 4 °C in the dark before Hg isotopes analysis. Hg isotopic compositions were measured by a multi – collector inductively coupled plasma mass spectrometer (MC-ICP-MS, Nu Instruments Ltd. UK) following the protocols presented in a previous study (Huang et al., 2018). Instrument mass bias was corrected using an internal standard (NIST 997 Tl) and strict sample-standard bracketing method (NIST 3133 Hg). The MDF of Hg (represented by δ-value, ‰) is defined by the following equation (Blum and Bergquist, 2007):

$$\delta^{xxx}Hg\ (‰) = [(^{xxx}Hg/^{198}Hg)_{sample}/(^{xxx}Hg/^{198}Hg)_{NIST\ 3133} - 1] \times 1000 \quad (1)$$

where xxx = 199, 200, 201, 202, and 204. The MIF of Hg (Δ-value, ‰) is calculated using the theoretically predicted MDF as the following equation (Blum and Bergquist,

https://doi.org/10.5194/acp-2021-493
Preprint. Discussion started: 6 July 2021

Atmospheric Chemistry and Physics Discussions

2007):

$$\Delta^{xxx}Hg\ (‰) = \delta^{xxx}Hg - (\delta^{202}Hg \times \beta) \quad (2)$$

where the mass-dependent scaling factor β is 0.252 for ^{199}Hg, 0.502 for ^{200}Hg, 0.752 for ^{201}Hg, and 1.493 for ^{204}Hg. A reference material UM-Almaden was measured repeatedly for quality control, yielding average $\delta^{202}Hg$ and $\Delta^{199}Hg$ values of -0.59 ± 0.10‰ (2σ, n = 25) and -0.03 ± 0.07‰ (2σ, n = 25), respectively. The results are well consistent with those in previous studies (Blum and Bergquist, 2007; Huang et al., 2015). The samples of this study were measured only once, so the 2σ uncertainties derived from repeated measurements of NIST 3133 standard during each analysis section were applied to the samples.

3. Results and discussion

3.1. Concentrations and isotopic compositions of $Hg_{PM2.5}$

Mass-based concentration of $Hg_{PM2.5}$ was used in this study to reflect reaction processes and isotopic fractionation. The mass concentrations and isotopes of $Hg_{PM2.5}$ at industrial and mountain sites are showed in Table 1. Average mass concentrations of $Hg_{PM2.5}$ using manual quartz filter were 0.52 ± 0.23 μg g^{-1} (0.15 to 1.10, n = 51) at the CX and 0.85 ± 0.63 μg g^{-1} (0.18 to 2.80, n = 33) at the DMS, respectively. A high $Hg_{PM2.5}$ concentration has been reported at the DMS before, which was likely due to regional Hg emissions (Yu et al., 2015). We found that the variation coefficient (VC = SD/Mean) of $Hg_{PM2.5}$ concentrations was lower at the CX (44.2%) than the DMS (74.1%). In addition, the volumetric concentrations of $PM_{2.5}$ and $Hg_{PM2.5}$ were correlated more closely at the CX (R^2 = 0.77, p < 0.01, n = 51) than the DMS (R^2 = 0.25, p < 0.01, n = 33). The data indicate that the DMS $Hg_{PM2.5}$ was influenced by diverse sources of $PM_{2.5}$ with different Hg levels and/or complex atmospheric Hg transformations. Spatial differences of $Hg_{PM2.5}$ were further examined by relationships of Hg with other chemical species in $PM_{2.5}$ (Table S1). In contrast to DMS, the mass concentrations of $Hg_{PM2.5}$ at the CX were well correlated to chemical tracers, like Cl^-, NO_3^-, K^+, and OC (r = 0.40 ~ 0.57, p < 0.05, Spearson correlation), implying the steady contributions of anthropogenic sources to $Hg_{PM2.5}$ in the industrial area.

$\delta^{202}Hg$ values for $Hg_{PM2.5}$ at the CX were in the range of -1.11‰ to 0.08‰ (mean:

https://doi.org/10.5194/acp-2021-493
Preprint. Discussion started: 6 July 2021


Atmospheric Chemistry and Physics Discussions

-0.61 ± 0.35‰, n = 10), while δ^{202}Hg values at the DMS were significantly higher and in a larger variation from -0.78‰ to 1.10‰ (mean: 0.12 ± 0.63‰, n = 10) ($p < 0.05$, *T* Test; Table 1 and Table S2). Hg_{PM} isotopic compositions in multiple types of locations are showed in Fig. 2 and Table S3. Negative δ^{202}Hg values are generally reported for PM in urban areas of China, such as Beijing, Changchun, Chengdu, Guiyang, and Xi'an (Mean: from -1.60‰ to -0.42‰; Huang et al., 2015, 2016, 2019, 2020; Xu et al., 2017, 2019; Yu et al., 2016), which are not distinguishable from those in remote areas. Moreover, δ^{202}Hg values for PM collected from urban and remote areas overlap those from nearby anthropogenic emissions (Das et al., 2016; Yu et al., 2016; Huang et al., 2018). In this study, the δ^{202}Hg values at the CX basically fell in the variation ranges mentioned above. Anthropogenic sources around the CX, such as industrial factories and coal fired power plant, were most likely the main drivers of negative MDF in $PM_{2.5}$ at this site. However, the slight positive δ^{202}Hg values at the DMS have seldom been reported in previous studies. There is no local anthropogenic emission sources around the DMS. Thus, some additional factors may cause positive shift of δ^{202}Hg values, although the magnitudes of them producing observed δ^{202}Hg are unclear. First, backward trajectory results show that $PM_{2.5}$ samples with positive δ^{202}Hg were generally associated with air masses coming or passing through the northeast of China (Fig. S1). An early study reported that coals in northern China have highest δ^{202}Hg value (-0.73 ± 0.33‰) compared to other regions in China (Yin et al., 2014b). Second, adsorption of gaseous Hg^{2+} on particles was suggested to be an important contributor to Hg_{PM} in the study region (Xu et al., 2020), so Hg_{PM} probably inherits significant positive MDF of Hg^{2+} (Rolison et al., 2013). The results suggest that the MDF of $Hg_{PM2.5}$ at the CX was dominantly affected by local anthropogenic sources, while the MDF at the DMS might be a mixed result of regional emissions and atmospheric transformations.

In contrast, Δ^{199}Hg values for $Hg_{PM2.5}$ at the two sites were not different ($p > 0.05$, *T* Test), with comparable values of 0.17 ± 0.22‰ (from -0.17‰ to 0.52‰) at the CX and 0.16 ± 0.24‰ (from -0.22‰ to 0.47‰) at the DMS, respectively. The Δ^{199}Hg values in this study are similar to those observed from remote areas in China (from

https://doi.org/10.5194/acp-2021-493
Preprint. Discussion started: 6 July 2021

Atmospheric Chemistry and Physics Discussions

0.27‰ to 0.66‰; Fu et al., 2019). A laboratory study indicated that photo-reduction of Hg^{2+} restrains odd Hg in reactants (aerosols here) in priority, which shifts $\Delta^{199}Hg$ values positively (Bergquist and Blum, 2007). As shown in Table S2 and Fig. S1, $PM_{2.5}$ samples affected by long range transport of air masses mostly had large positive $\Delta^{199}Hg$, like $PM_{2.5}$ collected on Apr. 4, 2018 from the CX and on Jan. 10, 2018 from the DMS. It's probably related to extensive photo-reduction of Hg^{2+} in aerosols during long range transport as previous studies suggested (Huang et al., 2016; Fu et al., 2019). Whereas, some $PM_{2.5}$ samples affected by local air masses were also characterized by significant positive $\Delta^{199}Hg$, like $PM_{2.5}$ collected on Apr. 4, 2018 from the CX. The remarkable odd-MIF of Hg_{PM} isotopes has commonly been reported in coastal environment (Rolison et al., 2013; Fu et al., 2019; Yu et al., 2020), thus the positive odd-MIF of $Hg_{PM2.5}$ in this study was likely contributed by enhanced photo-reactions. In addition, the MIF of ^{200}Hg, most probably relating to photo-reactions, was significant positive and displayed no spatial difference (0.11 ± 0.07‰ at the CX and 0.14 ± 0.07‰ at the DMS; $p > 0.05$, T Test), which also suggests enhanced and homogeneous photo-reactions in the study region. It is worth noting that a part of $PM_{2.5}$ samples collected from the DMS displayed negative $\delta^{202}Hg$ and near-zero $\Delta^{199}Hg$, similar to those from the CX (Fig. 2). Compared with the previous study (Yu et al., 2016), our results provide isotopes evidence that $Hg_{PM2.5}$ at the DMS was affected by multiple sources and one of them might be regional anthropogenic emissions.

Table 1 Mass concentrations and isotopic compositions of $Hg_{PM2.5}$ at the industrial site (CX) and mountain site (DMS) in East China

Parameter [a]	CX		DMS	
	Mean ± sd	Range	Mean ± sd	Range
$Hg_{PM2.5}$ (μg g^{-1})	0.52 ± 0.23	0.15 ~ 1.10	0.85 ± 0.63	0.18 ~ 2.80
$\delta^{202}Hg$ (‰)	-0.61 ± 0.35	-1.11 ~ 0.08	0.12 ± 0.63	-0.78 ~ 1.10
$\Delta^{199}Hg$ (‰)	0.17 ± 0.22	-0.17 ~ 0.52	0.16 ± 0.24	-0.22 ~ 0.47
$\Delta^{201}Hg$ (‰)	0.21 ± 0.18	-0.07 ~ 0.48	0.23 ± 0.36	-0.29 ~ 0.66
$\Delta^{200}Hg$ (‰)	0.11 ± 0.07	-0.01 ~ 0.23	0.14 ± 0.07	0.06 ~ 0.28
$\Delta^{204}Hg$ (‰)	0.19 ± 0.36	-0.16 ~ 0.93	3.58 ± 3.68	0.26 ~ 11.38

[a] 51 samples collected from CX and 32 samples from DMS for $Hg_{PM2.5}$ concentration analysis; 10

https://doi.org/10.5194/acp-2021-493
Preprint. Discussion started: 6 July 2021

Atmospheric Chemistry and Physics Discussions

315 samples from each site for isotope analysis.

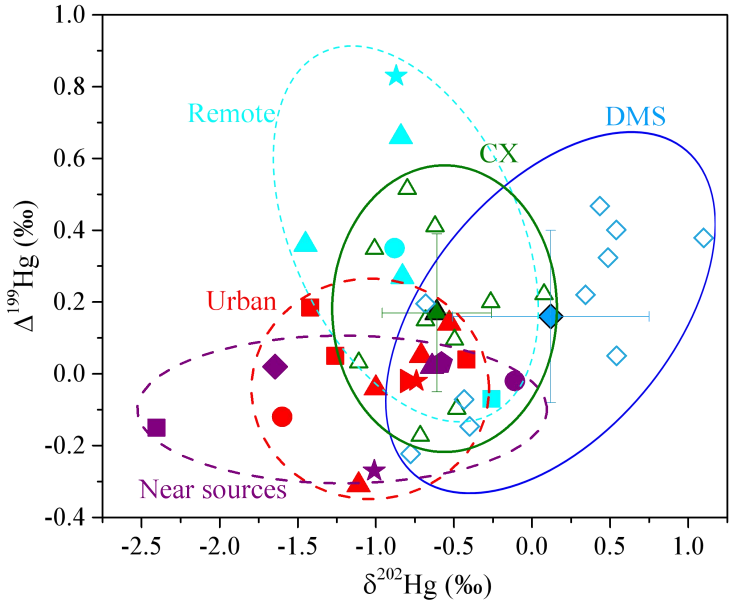

316

317 **Fig. 2** Isotopic compositions of Hg_{PM} at the multiple types of sites
318 (This study: ▲△mean and each values at the CX, ◆◇mean and each values at the DMS;
319 Remote sites: ★coast, ■▲mountain, ●island (Rolison et al., 2013; Yu et al., 2016; Fu et al.,
320 2019); Urban sites in China: ▲Beijing, ●Changchun, ★Chengdu, ■Guiyang, ▶Xi'an (Huang
321 et al., 2015, 2016, 2019, 2020; Xu et al., 2017, 2019; Yu et al., 2016); Sites near emission sources:
322 ▲■industrial, ●volcano, ⬟landfill, ◆traffic, ★near CFPP (Das et al., 2016; Huang et al., 2018;
323 Yu et al., 2016; Zambardi et al., 2009)

324 ***3.2. Influence of anthropogenic emissions on MDF of $Hg_{PM2.5}$***

325 Prior studies have compiled Hg isotopic compositions of major source materials,
326 such as fossil fuels, non-ferrous metal ores, and crustal rocks, and they generally
327 display large negative $\delta^{202}Hg$ and negative or near-zero $\Delta^{199}Hg$ values (Huang et al.,
328 2016; Sun et al., 2016). Combustion or/and industrial processing induces limited MIF
329 (Sun et al., 2013; Sun et al., 2016), so we assumed that emitted Hg conserves odd-Hg
330 isotopes of source materials. The $\Delta^{199}Hg$ values for most $Hg_{PM2.5}$ are distinguishable
331 from those of source materials, indicating that anthropogenic emissions were not the
332 drive factors for odd-MIF of $Hg_{PM2.5}$ in the study region. As for MDF, above analyses
333 indicated that the MDF of $Hg_{PM2.5}$ at the CX is subjected to local anthropogenic
334 sources, while the MDF at the DMS is probably caused by the combination of
335 atmospheric transformations and regional emissions. Spearson correlation between

https://doi.org/10.5194/acp-2021-493
Preprint. Discussion started: 6 July 2021


Atmospheric Chemistry and Physics Discussions

336 δ^{202}Hg and chemical components was conducted to explore the impacts of
337 anthropogenic emissions on $Hg_{PM2.5}$. The study region is highly industrialized, thus
338 industrial emissions are likely important contributors to $Hg_{PM2.5}$ isotopes. It's a pity
339 that we did not measure metallic elements to trace industrial contributions. As shown
340 in Table S4, the δ^{202}Hg values were associated with Cl^-, SO_4^{2-}, and levoglucosan
341 contents in $PM_{2.5}$, which are generally considered as indicatives of coal combustion
342 and biomass burning.

343 ***(1) Coal combustion***

344 Coal combustion was considered to be the primary Hg emission source in China,
345 which accounted for 47.2% of total anthropogenic emissions (253.8 t out of 537.8 t).
346 Coal combustion was also the dominant Hg emission source in Zhejiang province,
347 with a contribution of ~50% to total Hg emissions (Zhang et al., 2015). Hg isotopic
348 compositions of coals in China have large variations in MDF with δ^{202}Hg values from
349 -2.36‰ to -0.14‰ (Biswas et al., 2008; Yin et al., 2014b). A prior study reported that
350 emitted Hg_{PM} has a shift of -0.5‰ relative to δ^{202}Hg of coal feeds (Sun et al., 2014).
351 Hence δ^{202}Hg values for Hg_{PM} emitted from coal combustion in China were estimated
352 to be -2.86‰ to -0.64‰. The δ^{202}Hg values at the CX basically overlap and slightly
353 shift to positive, while the δ^{202}Hg values at the DMS have a large positive shift as
354 compared to those for emitted Hg_{PM} from coal combustion.

355 In this study, Cl^- was mainly originated from coal combustion, given that Cl^-
356 content in $PM_{2.5}$ was not correlated to Na^+. Besides, SO_4^{2-} was primarily transformed
357 from SO_2 which is mainly emitted from coal combustion. The δ^{202}Hg values at the CX
358 were significantly correlated to Cl^- content (R^2 = 0.46, P < 0.05, Fig. 3a) and well
359 associated with SO_4^{2-} content in $PM_{2.5}$ (R^2 = 0.38, P = 0.056, Fig. 3b). The results
360 imply that coal combustion played an important role in the MDF of $Hg_{PM2.5}$ at the CX.
361 It should be noted that there are many metal smelting factories near the CX. We did
362 not measure the tracers for smelting, but a previous study reported mean δ^{202}Hg value
363 for non-ferrous metal ores as -0.47 ± 0.77‰ (Yin et al., 2016). We assumed that Hg
364 emitted from non-ferrous metal smelting conserves the isotopes of source materials
365 due to lack of data for processing at current stage (Sun et al., 2016). Then, less

https://doi.org/10.5194/acp-2021-493
Preprint. Discussion started: 6 July 2021


Atmospheric Chemistry and Physics Discussions

366 negative MDF of Hg from non-ferrous metal smelting could explain the positive-shift
367 MDF at the CX relative to coal combustion emissions. It is reasonably inferred that
368 the MDF of $Hg_{PM2.5}$ at the CX is a result of multiple anthropogenic sources such as
369 coal combustion and non-ferrous metal smelting. Differently from the CX, the $\delta^{202}Hg$
370 values at the DMS were significantly correlated to SO_4^{2-} ($R^2 = 0.68$, $P < 0.05$, Fig. 3b),
371 but not to Cl^- ($P > 0.05$). It seems unlikely that coal combustion was the predominant
372 contributor to the positive MDF at the DMS. Whereas under the influence of transport,
373 the transformation of SO_2 to SO_4^{2-} usually enhances and the photo-reduction of Hg^{2+}
374 in aerosols tends to extensive which would shift $\delta^{202}Hg$ to positive to a certain extent
375 (Bergquist and Blum, 2007). The results imply that coal combustion emissions in a
376 regional scale or from long range transport had a potential impact on the MDF of
377 $Hg_{PM2.5}$ at the DMS, which is consistent with an earlier study conducted at the same
378 site based on Hg concentration and trajectory analysis (Yu et al., 2015).

379 ***(2) Biomass burning***

380 Total Hg emissions from biomass burning were estimated to be 3 ~ 4 t (Zhang et
381 al., 2015), which is very small relative to coal combustion. Whereas during some
382 times, like autumn harvesting and spring wildfire occurring seasons, biomass burning
383 could become a major contributor to atmospheric Hg (Giglio et al., 2013; Huang et al.,
384 2016; Fu et al., 2018). Previous studies have reported that biological materials display
385 negative $\delta^{202}Hg$ and $\Delta^{199}Hg$ values, like foliage ($\delta^{202}Hg$: -2.67‰ to -1.79‰; $\Delta^{199}Hg$:
386 -0.47‰ to -0.06‰), litterfall samples ($\delta^{202}Hg$: -3.03‰ to -2.35‰; $\Delta^{199}Hg$: -0.44‰ to
387 -0.22‰), and lichen ($\delta^{202}Hg$: -2.32‰ to -1.83‰; $\Delta^{199}Hg$: -0.35‰ to -0.22‰) (Demers
388 et al., 2013; Jiskra et al., 2015; Yin et al., 2013; Yu et al., 2016; Zheng et al., 2016).
389 Such negative $\delta^{202}Hg$ and $\Delta^{199}Hg$ of biological materials can not explain the isotopes
390 of $Hg_{PM2.5}$ in this study. Moreover, the contribution of biomass burning is supposed to
391 shift $\Delta^{199}Hg$ values negative, but we found no significant negative correlation between
392 $\Delta^{199}Hg$ and K^+ or levoglucosan as indicative of biomass burning influence from the
393 whole study period (Table S4). The results suggest that biomass burning was not the
394 dominant contributor to $Hg_{PM2.5}$ in the study region.

395 Interestingly, we found a close negative correlation between $\delta^{202}Hg$ and

https://doi.org/10.5194/acp-2021-493
Preprint. Discussion started: 6 July 2021

Atmospheric Chemistry and Physics Discussions

levoglucosan content in $PM_{2.5}$ at the CX (R^2 = 0.67, P < 0.05, Fig. 3c) excluding a $PM_{2.5}$ sample collected on Dec. 19, 2017. Considering no relevant study on Hg isotopic fractionation during burning processes so far, it can be assumed that Hg emitted from biomass burning conserves large negative MDF signature of biological materials. Thus, we cannot rule out the possibility that the contribution of biomass burning led to a negative deviation of δ^{202}Hg values at the CX to some extent. Actually, the contribution of biomass burning to $Hg_{PM2.5}$ is often substantial in a short time period (i.e., Mar. 2018, Fig. S2a, *https://firms.modaps.eosdis.nasa.gov/*), which can explain a weak correlation between Δ^{199}Hg and K^+ or levoglucosan in $PM_{2.5}$. In this study, the most negative odd-MIF was observed for $PM_{2.5}$ samples collected on Mar. 21, 2018, with Δ^{199}Hg value of -0.17‰ at the CX and -0.22‰ at the DMS. The finding was likely related to biomass burning, since those $PM_{2.5}$ samples were associated with air masses originating from or passing through the northeast of China with dense fire spots (Fig. S2b).

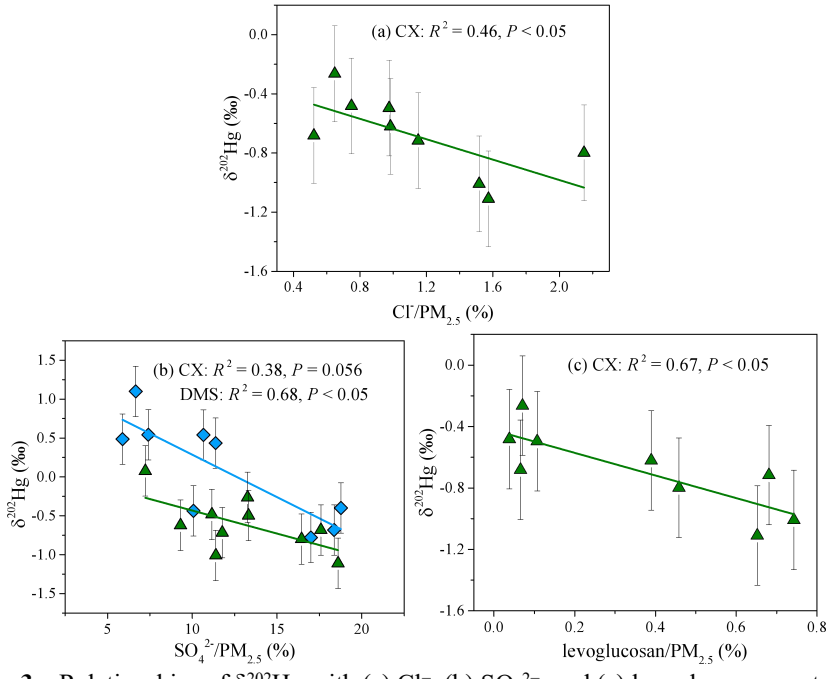

Fig. 3 Relationships of δ^{202}Hg with (a) Cl^-, (b) SO_4^{2-}, and (c) levoglucosan contents in $PM_{2.5}$ at CX (▲) or DMS (◆). Uncertainty (2σ) for δ^{202}Hg in $PM_{2.5}$ is 0.25‰.

3.3. Influence of photo-chemical process on isotopes of $Hg_{PM2.5}$

https://doi.org/10.5194/acp-2021-493
Preprint. Discussion started: 6 July 2021


Atmospheric Chemistry and Physics Discussions

Large odd-MIF of Hg isotopes in most $PM_{2.5}$ samples of this study was likely related to photo-chemical processes. An experiment study has found that the oxidation of Hg^0 by halogen atom (Cl· or Br·) results in a negative shift of $\Delta^{199}Hg$ in product Hg^{2+} (Sun et al., 2016). Given that partitioning of Hg^{2+} between gas and particle phases leads to limited odd-MIF of Hg isotopes (Wiederhold et al., 2010, Fu et al., 2019), then the formation of Hg_{PM} via oxidation of Hg^0 and following adsorption on particles could not explain the positive odd-MIF of $Hg_{PM2.5}$ in this study. Previous experiments and field studies have reported that photo-reduction of Hg^{2+} in aqueous solution induces the odd-MIF of Hg isotopes and results in large positive $\Delta^{199}Hg$ values (Bergquist and Blum, 2007; Zheng and Hintelmann, 2009, 2010). Hence, photo-reduction of inorganic Hg^{2+} in aerosols could be proposed to be a key factor for the odd-MIF of $Hg_{PM2.5}$ in the study region. The linear relationship between $\Delta^{199}Hg$ and $\Delta^{201}Hg$ is often used to identify MIF processes of odd-Hg isotopes. The slope of $\Delta^{199}Hg$ versus $\Delta^{201}Hg$ yielded from overall data was 0.92 in this study ($R^2 = 0.83$, $P < 0.01$; Fig. 4a). The near-unity slope of $\Delta^{199}Hg$ versus $\Delta^{201}Hg$ was widely observed in particles from other studies (Rolison et al., 2013; Huang et al., 2016, 2019; Fu et al., 2019; Xu et al., 2019). The $\Delta^{199}Hg/\Delta^{201}Hg$ ratio of this study is consistent with the indicative ratio of aqueous photo-reduction of inorganic Hg^{2+} (~1.0, Bergquist and Blum, 2007; Zheng and Hintelmann, 2009), but different from the ratios of other processes, like photo-oxidation (1.64 by Br· and 1.89 by Cl·, Sun et al., 2016) and photo-demethylation (1.36, Bergquist and Blum, 2007). Isotopic compositions of Hg_{PM} are usually the combined effects of many environmental processes, like above mentioned photo-reactions and various anthropogenic sources. Thus, the observed odd-MIF of $Hg_{PM2.5}$ in the study region seems like a "net" result of aqueous photo-reduction process.

The similarity of odd-MIF anomaly between the CX and DMS suggests the photo-reduction of Hg^{2+} in aerosols was homogeneous on a regional scale. However, relationships of $\Delta^{199}Hg$ with $Hg_{PM2.5}$ content and $\delta^{202}Hg$ showed distinct spatial difference. For the DMS, the $\Delta^{199}Hg$ values generally decreased with $Hg_{PM2.5}$ content increased (Fig. 4b) and the correlation between $\Delta^{199}Hg$ and $\delta^{202}Hg$ was significantly

https://doi.org/10.5194/acp-2021-493
Preprint. Discussion started: 6 July 2021

Atmospheric Chemistry and Physics Discussions

445 positive (R^2 = 0.56, P < 0.05; Fig. 4c). Experimental studies have indicated that the
446 photo-reduction of Hg^{2+} releases Hg^0 and preferentially retains odd and heavier
447 isotopes in solutions (Bergquist and Blum, 2007; Zheng and Hintelmann, 2009),
448 which is expected to result in a positive relationship between Δ^{199}Hg and δ^{202}Hg and
449 an inverse relationship between Δ^{199}Hg and $Hg_{PM2.5}$ content. In this study, the
450 consistent relationships of Δ^{199}Hg with δ^{202}Hg and $Hg_{PM2.5}$ at the DMS strongly imply
451 a predominant role of photo-reduction in isotopic fractionation of $Hg_{PM2.5}$ at this site.
452 In addition, δ^{202}Hg signatures of anthropogenic emissions from regional and
453 long-range transport might be largely obscured by photo-reduction process, which
454 well explains the positive δ^{202}Hg at the DMS. In contrast, the variation of Δ^{199}Hg at
455 the CX was not associated with $Hg_{PM2.5}$ contents or δ^{202}Hg. The result suggests an
456 insignificant impact of photo-reduction relative to anthropogenic sources on MDF and
457 Hg content in $PM_{2.5}$ at the CX. On the other hand, a better coincidence of high $Hg_{PM2.5}$
458 and high δ^{202}Hg (Fig. 4d) supports that constant local Hg emissions dominantly
459 affected $Hg_{PM2.5}$ content at the CX.

460

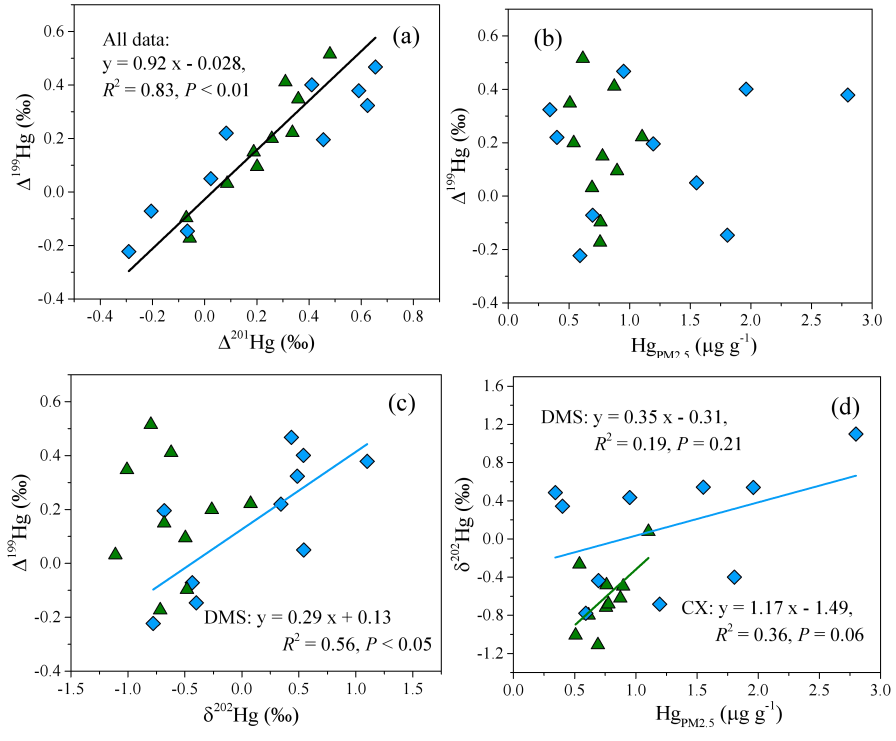

461

https://doi.org/10.5194/acp-2021-493
Preprint. Discussion started: 6 July 2021


Atmospheric Chemistry and Physics Discussions

462 **Fig. 4** Linear relationships between (a) Δ^{199}Hg and Δ^{201}Hg, (b) Δ^{199}Hg and $Hg_{PM2.5}$
463 content, (c) Δ^{199}Hg and δ^{202}Hg, and (d) δ^{202}Hg and $Hg_{PM2.5}$ content at the CX (▲) and
464 DMS (◆). Uncertainty (2σ) for Δ^{199}Hg and δ^{202}Hg in $PM_{2.5}$ is 0.03‰ and 0.25‰,
465 respectively.

466 ***3.4. Potential mechanism of even-MIF***

467 A small but significant MIF of ^{200}Hg was observed in most $PM_{2.5}$ samples from
468 this study, with mean Δ^{200}Hg values of 0.11 ± 0.07‰ at the CX and 0.14 ± 0.07‰ at
469 the DMS. They are more positive than those in urban (mean = 0.01‰ to 0.09‰, Das
470 et al., 2016; Huang et al., 2016; Xu et al., 2017) and remote areas (mean = 0.07‰ to
471 0.10‰, Fu et al., 2019), but similar to those in coastal and island areas (Rolison et al.,
472 2013; Fu et al., 2019). In general, Hg emitted from anthropogenic sources has Δ^{200}Hg
473 of near-zero (Sun et al., 2016b), while large Δ^{200}Hg values are mainly observed in
474 atmospheric samples, i.e., precipitation, gaseous Hg^{2+}, and aerosols (Chen et al., 2012;
475 Rolison et al., 2013; Fu et al., 2019). Significant even-MIF of Hg isotopes has been
476 suggested to associate with photo-oxidation of Hg^0, from upper troposphere or/and
477 from in situ involving UV light and oxidants (Chen et al., 2012; Fu et al., 2019). This
478 could help explain significant Δ^{200}Hg values in coastal areas where halogen atoms are
479 expected to be abundant. The Δ^{200}Hg values in $PM_{2.5}$ were not different between sites,
480 similar to Δ^{199}Hg values, which supports that the observed Δ^{200}Hg were associated
481 with photo-chemical processes of minor spatial difference.

482 An experimental study showed that gas-phase oxidation of Hg^0 vapor by Cl and
483 Br atoms results in positive Δ^{200}Hg and large negative Δ^{199}Hg values in products (Sun
484 et al., 2016a). So direct oxidation of Hg^0 in particles could explain positive Δ^{200}Hg but
485 positive Δ^{199}Hg values in this study. Based on previous field and experimental studies,
486 we can preferably hypothesize several phases during Hg_{PM} transformations. (1)
487 gas-phase oxidation of Hg^0. This process generally enhances in areas with abundant
488 halogen atoms (Wang et al., 2019), which would result in detectable positive Δ^{200}Hg
489 values in products (gaseous Hg^{2+}) (Sun et al., 2016a). (2) gas-particle partitioning of
490 Hg^{2+}. This process made an important contribution to Hg_{PM} in the study region (Xu et
491 al., 2020), but it is strongly temperature-dependent that unlikely produces the MIF of
492 Hg isotopes (Fu et al., 2019). (3) aqueous photo-reduction of Hg^{2+} in particles. This

https://doi.org/10.5194/acp-2021-493
Preprint. Discussion started: 6 July 2021


Atmospheric Chemistry and Physics Discussions

process induces positive odd-MIF of Hg isotopes as previously discussed. The proposed speculation can basically explain for Δ^{199}Hg and Δ^{200}Hg values in coastal and island areas, although there are still some uncertainties, like fractionation of Hg isotopes during gas-particle partitioning.

The MIF of ^{204}Hg has only been reported in a few studies, presenting small positive values for TGM and negative values in precipitation and remote PM samples (Demers et al., 2013, 2015; Fu et al., 2019). Interesting, we observed a distinct spatial difference in Δ^{204}Hg values, with 3.58 ± 3.68‰ (from 0.26‰ to 11.38‰) at the DMS and 0.19 ± 0.36‰ at the CX (lower than 2SD of repeated NIST 3177 analysis). The large positive Δ^{204}Hg at the DMS have not been reported in atmospheric samples before. In addition, there was no correlation between Δ^{204}Hg and Δ^{200}Hg in this study, which is not consistent with the early finding that Δ^{204}Hg values were complementary to Δ^{200}Hg (Demers et al., 2013; Fu et al., 2019). It's generally speculated that even-MIF of Hg isotopes is derived from photo-oxidation of Hg^0 to Hg^{2+} (Chen et al., 2012). However, the difference in spatial distribution for Δ^{200}Hg and Δ^{204}Hg in this study not very support this speculation. Up to now, the mechanisms for even-MIF of Hg isotopes remain unknown and we can not give a further explanation for Δ^{204}Hg in $PM_{2.5}$ in this study.

3.5. Isotopes of Hg in adjacent surface seawater

Hg isotopes are often used to track the transport and transformations of Hg in the environment. The average concentration of THg in seawater was 10.5 ± 5.0 ng L^{-1}, with a range of 1.9 ~ 23.6 ng L^{-1} (Table S1). As shown in Fig. 5, the concentrations of seawater THg displayed distinct time variations, with higher levels during Sep. ~ Mar. than during Apr. ~ Aug, which is likely related to precipitation cycle. The average δ^{202}Hg value of seawater samples was -1.31 ± 0.59‰, with most samples fell in the range of -2.00‰ ~ -1.00‰. Whereas Hg-MIF in seawater samples was not significant, with mean Δ^{199}Hg, Δ^{201}Hg, and Δ^{200}Hg values of -0.02 ± 0.07‰, 0.00 ± 0.05‰, and 0.04 ± 0.03‰, respectively. The negative MDF and near-zero MIF of surface seawater are well consistent with those of source materials (Huang et al., 2016; Sun et al., 2016b), suggesting the dominant effect of anthropogenic emissions on Hg in offshore

https://doi.org/10.5194/acp-2021-493
Preprint. Discussion started: 6 July 2021

Atmospheric Chemistry and Physics Discussions

surface seawater. A minor change in intensity of industrial activities as expected among the months also supports the above deduction.

Isotopic compositions of THg in surface seawater and Hg_{PM} at the adjacent industrial site are consistent in MDF but not in MIF. Similar results were obtained when comparing to wet deposition which presents negative $\delta^{202}Hg$ and positive $\Delta^{199}Hg$ and $\Delta^{200}Hg$ (Chen et al., 2012; Huang et al., 2018). Negative MDF of Hg in industrial $PM_{2.5}$ and adjacent surface seawater implies an important role of local anthropogenic sources. On the other hand, the unity slope of $\Delta^{199}Hg$ versus $\Delta^{201}Hg$ ($\Delta^{199}Hg = 1.12 \times \Delta^{201}Hg - 0.02$, $R^2 = 0.68$, n = 19) indicates that the odd-MIF of Hg isotopes in surface seawater was mainly produced by photo-reduction of Hg^{2+}. Whereas, the minor $\Delta^{199}Hg$ anomalies suggest that photo-reduction was not evident for surface seawater. A big discrepancy in the MIF of Hg isotopes between atmospheric samples and surface seawater further evidences that atmospheric transformations would induce significant MIF of Hg isotopes, which obscures Hg isotopic signatures of anthropogenic emissions.

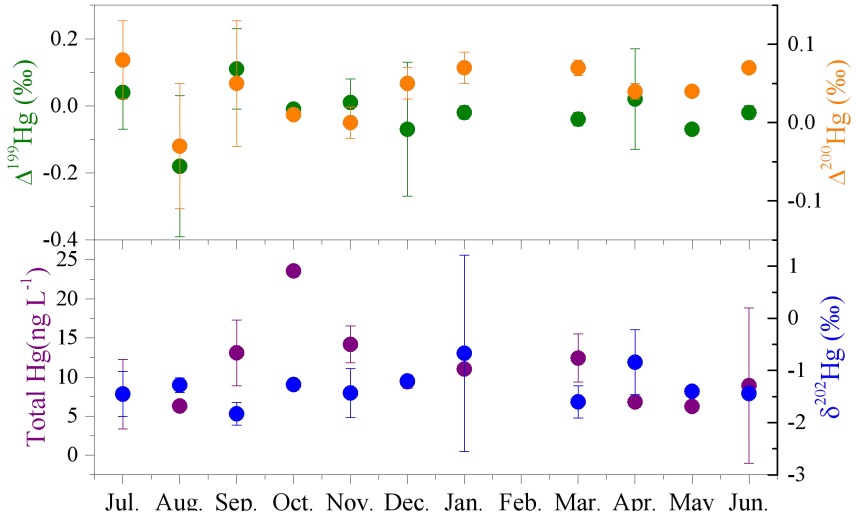

Fig. 5 Monthly variations of total Hg concentration, $\delta^{202}Hg$, $\Delta^{199}Hg$ and $\Delta^{200}Hg$ of surface seawater during the sampling period from July 2017 to June 2018

4. Conclusion

This study investigated Hg isotopic compositions in $PM_{2.5}$ collected from nearby industrial and mountain sites in a coastal area and also in adjacent offshore surface

https://doi.org/10.5194/acp-2021-493
Preprint. Discussion started: 6 July 2021


Atmospheric Chemistry and Physics Discussions

seawater. $Hg_{PM2.5}$ displayed significant spatial difference in MDF but not in odd-MIF. Negative $\delta^{202}Hg$ in $PM_{2.5}$ at the CX was primarily induced by local industrial activities like coal combustion. Whereas, the slight positive $\delta^{202}Hg$ at the DMS could not be fully explained by anthropogenic emissions. Other than the effect of regional transport, a close correlation between $\delta^{202}Hg$ and $\Delta^{199}Hg$ at the DMS implies that photo-chemical processes likely contributed to the MDF of $Hg_{PM2.5}$. Significant positive odd-MIF of $Hg_{PM2.5}$ and the unity slope of $\Delta^{199}Hg$ versus $\Delta^{201}Hg$ indicate an important role of photo-reduction in aerosols. The observed positive $\Delta^{200}Hg$ values in this study were probably associated with photo-oxidation of Hg^0 which is generally enhanced in the coastal environment. THg in surface seawater was characterized by negative MDF and near-zero odd-MIF, which is more consistent with isotopic signatures of source materials. The anomalies of Hg-MIF were larger for atmospheric $PM_{2.5}$ than for surface seawater, suggesting that atmospheric transformations induce significant MIF of Hg isotopes and obscure Hg isotopic signatures of initial emissions. This study illustrates that the comparison of Hg isotopic compositions among relevant media is more effective to identify Hg emission sources and atmospheric transformations.

Novelty statement

Comparison of isotopic compositions of $Hg_{PM2.5}$ was conducted between nearby industrial and mountain sites, which is more effective to reveal the roles of anthropogenic emission sources and transformation processes in varying Hg isotopes. Hg isotopic compositions in industrial $PM_{2.5}$ and in offshore surface seawater were also compared. The results indicate that atmospheric transformations would induce significant fractionation of Hg isotopes and obscure the specific Hg isotopic signatures of initial emissions.

Data availability. HYSPLIT trajectory model and gridded meteorological data (Global Data Assimilation System, GDAS1) are available from the US National Oceanic and Atmospheric Administration (http://ready.arl.noaa.gov). Fire data are

https://doi.org/10.5194/acp-2021-493
Preprint. Discussion started: 6 July 2021


Atmospheric Chemistry and Physics Discussions

574 available in the Fire Information for Resource Management System (FIRMS,
575 https://firms2.modaps.eosdis.nasa.gov/map/#d:2021-04-26..2021-04-27;@6.7,2.0,3z).
576 All data in this study are available upon request to the first author via email
577 (linglingxu@iue.ac.cn).
578
579 **Author contributions**. JSC, LLX, and YRZ designed this study. MRL, LQY, YTC,
580 LT and HX conducted the sampling. YRZ and LLX participated in sample treatment
581 and measurements. LLX wrote the paper. JYS and YPC helped the graphics
582 production. All authors reviewed the paper.
583
584 **Competing interests.** The authors declare that they have no conflict of interest.
585
586 **Acknowledgements.** This research was financially supported by National Natural
587 Science Foundation of China (No. 21507127; 41575146 & U1405235), Natural
588 Science Foundation of Fujian province (2016J05050), the Cultivating Project of
589 Strategic Priority Research Program of Chinese Academy of Sciences (XDPB1903),
590 the CAS Center for Excellence in Regional Atmospheric Environment (E0L1B20201),
591 and Xiamen Atmospheric Environment Observation and Research Station of Fujian
592 Province.
593
594 **References**
595 Bergquist, B. A. and Blum, J. D.: Mass-dependent and -independent fractionation of
596 Hg isotopes by photoreduction in aquatic systems, Science, 318, 417−420, doi:
597 10.1126/science.1148050, 2007.
598 Bergquist, R. A. and Blum, J. D.: The odds and evens of mercury isotopes:
599 applications of mass-dependent and mass-independent isotope fractionation,
600 Elements, 5(6), 353−357, doi: 10.2113/gselements.5.6.353, 2009.

https://doi.org/10.5194/acp-2021-493
Preprint. Discussion started: 6 July 2021


Atmospheric Chemistry and Physics Discussions

601 Biswas, A., Blum, J. D., Bergquist, B. A., Keeler, G. J., Xie, Z. Q.: Natural mercury
602 isotope variation in coal deposits and organic soils, Environ. Sci. Technol.,
603 42(22), 8303−8309, doi: 10.1021/es801444b, 2008.
604 Blum, J. D. and Bergquist, R. A.: Reporting of variations in the natural isotopic
605 composition of mercury, Anal. Bioanal. Chem., 338(2), 353–359, doi:
606 org/10.1007/s00216-007-1236-9, 2007.
607 Blum, J. D., Sherman, L. S., Johnson, M. W.: Mercury isotopes in earth and
608 environmental sciences, Annu. Rev. Earth Planet. Sci., 42, 249–269, doi:
609 10.1146/annurev-earth-050212-124107, 2014.
610 Blum, J. D. and Johnson, M. W.: Recent developments in mercury stable isotope
611 analysis, Non-Traditional Stable Isotopes, 82, 733-757, doi:
612 10.2138/rmg.2017.82.17, 2017.
613 Carignan, J., Estrade, N., Sonke, J. E., Donard, O. F. X.: Odd isotope deficits in
614 atmospheric Hg measured in lichens, Environ. Sci. Technol., 43(15), 5660-5664,
615 doi: 10.1021/es900578v, 2009.
616 Chen, J. B., Hintelmann, H., Feng, X. B., Dimock, B.: Unusual fractionation of both
617 odd and even mercury isotopes in precipitation from Peterborough, ON, Canada,
618 Geochim. Cosmochim. Ac., 90, 33−46, doi: 10.1016/j.gca.2012.05.005, 2012.
619 Das, R., Wang, X. F., Khezri, B., Webster, R. D., Sikdar, P. K., Datta, S.: Mercury
620 isotopes of atmospheric particle bound mercury for source apportionment study
621 in urban Kolkata, India, Elementa-Sci. Anthrop., 4, 1−12, doi: 10.12952/journal.
622 elementa.000098, 2016.
623 Demers, J. D., Blum, J. D., Zak, D. R.: Mercury isotopes in a forested ecosystem:
624 Implications for air-surface exchange dynamics and the global mercury cycle,
625 Global Biogeochem. Cy., 27(1), 222−238, doi: 10.1002/gbc.20021, 2013.
626 Demers, J. D., Sherman, L. S., Blum, L. S., Marsik, F. J., Dvonch, J. T.: Coupling
627 atmospheric mercury isotope ratios and meteorology to identify sources of
628 mercury impacting a coastal urban-industrial region near Pensacola, Florida,

https://doi.org/10.5194/acp-2021-493
Preprint. Discussion started: 6 July 2021


Atmospheric Chemistry and Physics Discussions

629 USA, Global Biogeochem. Cy., 29(10), 1689−1705, doi: 10.1002/2015gb005146,
630 2015.
631 Fu, X. W., Zhang, H., Yu, B., Wang, X., Lin, C.-J., and Feng, X. B.: Observations of
632 atmospheric mercury in China: a critical review, Atmos. Chem. Phys., 15, 9455−
633 9476, doi:10.5194/acp-15-94552015, 2015.
634 Fu, X. W., Marusczak, N., Wang, X., Gheusi, F., Sonke, J. E.: Isotopic Composition of
635 Gaseous Elemental Mercury in the Free Troposphere of the Pic du Midi
636 Observatory, France, Environ. Sci. Technol., 50(11), 5641-5650,
637 doi:10.1021/acs.est.6b00033, 2016.
638 Fu, X. W., Yang, X., Tan, Q. Y., Ming, L. L., Lin, T., Lin, C.-J., Li, X. D., Feng, X. B.:
639 Isotopic composition of gaseous elemental mercury in the marine boundary layer
640 of East China Sea, J. Geophys. Res.: Atmos., 123, 7656 − 7669, doi:
641 10.1029/2018JD028671, 2018.
642 Fu, X. W., Zhang, H., Feng, X. B., Tan, Q. Y., Ming, L. L., Liu, C., Zhang, L. M.:
643 Domestic and transboundary sources of atmospheric particulate bound mercury
644 in remote areas of China: Evidence from mercury isotopes, Environ. Sci.
645 Technol., 53(4), 1947−1957, doi: 10.1021/acs.est.8b06736, 2019.
646 Giglio, L., Randerson, J. T., van der Werf, G. R.: Analysis of daily, monthly, and
647 annual burned area using the fourth-generation global fire emissions database
648 (GFED4), J. Geophys. Res.: Biogeosci, 118 (1), 317−328, doi:
649 10.1002/jgrg.20042, 2013.
650 Gratz, L. E., Keeler, G. J., Blum, J. D., Sherman, L. S.: Isotopic composition and
651 fractionation of mercury in Great Lakes precipitation and ambient air, Environ.
652 Sci. Technol., 44(20), 7764-7770, doi: 10.1021/es100383w, 2010.
653 Horowitz, H. M., Jacob, D. J., Zhang, Y. X., Dibble, T. S., Slemr, F., Amos, H. M.,
654 Schmidt, J. A., Corbitt, E. S., Marais, E. A., Sunderland, E. M.: A new
655 mechanism for atmospheric mercury redox chemistry: implications for the global

https://doi.org/10.5194/acp-2021-493
Preprint. Discussion started: 6 July 2021


Atmospheric Chemistry and Physics Discussions

mercury budget, Atmos. Chem. Phys., 17(10), 6353 − 6371, doi: org/10.5194/acp-17-6353-2017, 2017.

Hong, Z. Y., Zhang, H., Zhang, Y. R., Xu, L. L., Liu, T. T., Xiao, H., Hong, Y. W., Chen, J. S., Li, M. R., Deng, J. J., Wu, X., Hu, B. Y., Chen, X. Q.: Secondary organic aerosol of PM2.5 in a mountainous forest area in southeastern China: Molecular compositions and tracers implication, Sci, Total Environ. 653: 496 − 503, doi: 10.1016/j.scitotenv.2018.10.370, 2019.

Huang, Q., Liu, Y. L., Chen, J. B., Feng, X. B., Huang, W. L., Yuan, S. L., Cai, H. M., Fu, X. W.: An improved dual-stage protocol to pre-concentrate mercury from airborne particles for precise isotopic measurement, J. Anal. Atom. Spectrom., 30(4), 957−966, doi: 10.1039/c4ja00438h, 2015.

Huang, Q., Chen, J. B., Huang, W. L., Fu, P. Q., Guinot, B., Feng, X. B., Shang, L. H., Wang, Z. H., Wang, Z. W., Yuan, S. L., Cai, H. M., Wei, L. F., Yu, B.: Isotopic composition for source identification of mercury in atmospheric fine particles, Atmos. Chem. Phys., 16(18), 11773–11786, doi:10.5194/acp-16-11773-2016, 2016.

Huang, Q., Chen, J. B., Huang, W. L., Reinfelder, J. R., Fu, P. Q., Yuan, S. L., Wang, Z. W., Yuan, W., Cai, H. M., Ren, H., Sun, Y. L., He, L.: Diel variation in mercury stable isotope ratios records photoreduction of PM2.5-bound mercury, Atmos. Chem. Phys., 19(1), 315−325, doi: 10.5194/acp-19-315-2019, 2019.

Huang, Q., Reinfelder, J. R., Fu, P. Q., Huang, W. L.: Variation in the mercury concentration and stable isotope composition of atmospheric total suspended particles in Beijing, China, J. Hazard. Mater., 383, 121131, doi: 10.1016/j.jhazmat. 2019.121131, 2020.

Huang, S. Y., Sun, L. M., Zhou, T. J., Yuan, D. X., Du, B., Sun, X. W.: Natural stable isotopic compositions of mercury in aerosols and wet precipitations around a coal-fired power plant in Xiamen, southeast China, Atmos. Environ., 173, 72−80, doi: 10.1016/j.atmosenv.2017.11.003, 2018.

https://doi.org/10.5194/acp-2021-493
Preprint. Discussion started: 6 July 2021


Atmospheric Chemistry and Physics Discussions

684 Jiskra, M., Wiederhold, J. G., Skyllberg, U., Kronberg, R. M., Hajdas, I., Kretzschmar,
685 R.: Mercury deposition and re-emission pathways in boreal forest soils
686 investigated with Hg isotope signatures, Environ. Sci. Technol., 49(12), 7188 –
687 7196, doi: 10.1021/acs.est.5b00742, 2015.
688 Malinovsky, D., Latruwe, K., Moens, L., Vanhaecke, F.: Experimental study of
689 mass-independence of Hg isotope fractionation during photodecomposition of
690 dissolved methylmercury, J. Anal. Atom. Spectrom., 25(7), 950-956, doi:
691 10.1039/b926650j, 2010.
692 Mao, H. T., Cheng, I., Zhang, L. M.: Current understanding of the driving
693 mechanisms for spatiotemporal variations of atmospheric speciated mercury: a
694 review, Atmos. Chem. Phys., 16(20), 12897-12924, doi:
695 10.5194/acp-16-12897-2016, 2016.
696 Rolison, J. M., Landing, W. M., Luke, W., Cohen, M., Salters, V. J. M.: Isotopic
697 composition of species-specific atmospheric Hg in a coastal environment, Chem.
698 Geol., 336, 37–49, doi: 10.1016/j.chemgeo.2012.10.007, 2013.
699 Schroeder, W. H. and Munthe J.: Atmospheric mercury — An overview, Atmos.
700 Environ., 32(5), 809–822, doi:10.1016/S1352-2310(97) 00293-8, 1998.
701 Sherman, L. S., Blum, J. D., Johnson, K. P., Keeler, G. J., Barres, J. A., Douglas, T. A.:
702 Mass-independent fractionation of mercury isotopes in Arctic snow driven by
703 sunlight, Nat. Geosci., 3(3), 173-177, doi: 10.1038/NGEO758, 2010.
704 Sonke, J. E. and Blum, J. D.: Advances in mercury stable isotope biogeochemistry
705 preface, Chem. Geol., 336, 1–4, doi: 10.1016/j.chemgeo.2012.10.035, 2013.
706 Sun, G. Y., Sommar, J., Feng, X. B., Lin, C.-J., Ge, M. F., Wang, W. G., Yin, R. S., Fu,
707 X. W., Shang, L. H.: Mass-dependent and -independent fractionation of mercury
708 isotope during gas-phase oxidation of elemental mercury vapor by atomic Cl and
709 Br, Environ. Sci. Telchnol., 50(17), 9232 – 9241, doi: 10.1021/acs.est.6b01668,
710 2016a.

https://doi.org/10.5194/acp-2021-493
Preprint. Discussion started: 6 July 2021

711 Sun, R. Y., Heimburger, L. E., Sonke, J. E., Liu, G. J.: Mercury stable isotope
712 fractionation in six utility boilers of two large coal-fired power plants, Chem.
713 Geol., 336, 103−111, doi: 10.1016/j.chemgeo.2012.10.055, 2013.
714 Sun, R. Y., Sonke, J. E., Heimburger, L. E., Belkin, H. E., Liu, G. J., Shome, D.,
715 Cukrowska, E., Liousse, C., Pokrovsky, O. S., Streets, D. G.: Mercury stable
716 isotope signatures of world coal deposits and historical coal combustion
717 emissions, Environ. Sci. Technol., 48(13), 7660−7668, doi: 10.1021/es501208a,
718 2014.
719 Sun, R. Y., Streets, D. G., Horowitz, H. M., Amos, H. M., Liu, G. J., Perrot, V.,
720 Toutain, J.P., Hintelmann, H., Sunderland, E. M., Sonke, J. E.: Historical
721 (1850-2010) mercury stable isotope inventory from anthropogenic sources to the
722 atmosphere, Elementa-Sci. Anthrop., 4, 1 − 15, doi:
723 10.12952/journal.elementa.000091, 2016b.
724 Wang, S. Y., McNamara, S. M., Moore, C. W., Obrist, D., Steffen, A., Shepson, P. B.,
725 Steabler, R. M., Raso, A. R. W., Pratt, K. A.: Direct detection of atmospheric
726 atomic bromine leading to mercury and ozone depletion, P. Natl. Acad. Sci.,
727 116(29), 14479−14484, doi: 10.1073/pnas.1900613116, 2019.
728 Xu, H. M., Sonke, J. E., Guinot, B., Fu, X. W., Sun, R. Y., Lanzanova, A., Candaudap,
729 F., Shen, Z. X., Cao, J. J.: Seasonal and annual variations in atmospheric Hg and
730 Pb isotopes in Xi'an, China, Environ. Sci. Technol., 51(7), 3759 − 3766, doi:
731 10.1021/acs.est.6b06145, 2017.
732 Xu, H. M., Sun, R. Y., Cao, J. J., Huang, R. J., Guinot, B., Shen, Z. X., Jiskra, M., Li,
733 C. X., Du, B. Y., He, C., Liu, S.X., Zhang, T., Sonke, J. E.: Mercury stable
734 isotope compositions of Chinese urban fine particulates in winter haze days:
735 Implications for Hg sources and transformations, Chem. Geol., 504, 267 − 275,
736 doi: 10.1016/j.chemgeo.2018.11.018, 2019.
737 Xu, L. L., Chen, J. S., Yang, L. M., Yin, L. Q., Yu, J. S., Qiu, T. X., Hong, Y.W.:
738 Characteristics of total and methyl mercury in wet deposition in a coastal city,

https://doi.org/10.5194/acp-2021-493
Preprint. Discussion started: 6 July 2021


Atmospheric Chemistry and Physics Discussions

739 Xiamen, China: Concentrations, fluxes and influencing factors on Hg
740 distribution in precipitation, Atmos. Environ. 99, 10 – 16, doi:
741 10.1016/j.atmosenv.2014.09.054, 2014.
742 Xu, L. L., Jiao, L., Hong, Z. Y., Zhang, Y. R., Du, W. J., Wu, X., Chen, Y. T., Deng, J.
743 J., Hong, Y. W., Chen, J. S.: Source identification of $PM_{2.5}$ at a port and an
744 adjacent urban site in a coastal city of China: Impact of ship emissions and port
745 activities, Sci. Total Environ., 634: 1205 – 1213, doi:
746 10.1016/j.scitotenv.2018.04.087, 2018.
747 Xu, L. L., Zhang, Y. R., Tong, L., Chen, Y. P., Zhao, G. Q., Hong, Y. W., Xiao, H.,
748 Chen, J. S.: Gas-particle partitioning of atmospheric reactive mercury and its
749 contribution to particle bound mercury in a coastal city of the Yangtze River
750 Delta, China, Atmos. Environ., 239, 117744, doi:
751 10.1016/j.atmosenv.2020.117744, 2020.
752 Yi, H., Tong, L., Lin, J. M., Cai, Q. L., Wang, K. Q., Dai, X. R., Li, J. R., Chen, J. S.,
753 Xiao, H.: Temporal variation and long-range transport of gaseous elemental
754 mercury (GEM) over a coastal site of East China, Atmos. Res., 233, 104699, doi:
755 10.1016/j.atmosres.2019.104699, 2020.
756 Yin, R. S., Feng, X. B., Meng, B.: Stable mercury isotope variation in rice plants
757 (Oryza sativa L.) from the Wanshan mercury mining district, SW China, Environ.
758 Sci. Technol., 47(5), 2238−2245, doi: 10.1021/es304302a, 2013.
759 Yin, R. S., Feng, X. B., Li, X. D., Yu, B., Du, B. Y.: Trends and advances in mercury
760 stable isotopes as a geochemical tracer, Trends Environ. Anal., 2, 1 – 10, doi:
761 10.1021/es500322n, 2014a.
762 Yin, R. S., Feng, X. B., Chen, J. B.: Mercury stable isotopic compositions in coals
763 from major coal producing fields in China and their geochemical and
764 environmental Implications, Environ. Sci. Technol., 48(10), 5565 – 5574, doi:
765 10.1021/es500322n, 2014b.

https://doi.org/10.5194/acp-2021-493
Preprint. Discussion started: 6 July 2021


Atmospheric Chemistry and Physics Discussions

766 Yin, R. S., Feng, X. B., Hurley, J. P., Krabbenhoft, D. P., Lepak, R. F., Hu, R. Z.,
767 Zhang, Q., Li, Z. G., Bi, X. W.: Mercury isotopes as proxies to identify sources
768 and environmental impacts of mercury in Sphalerites, Sci. Rep., 6, 2045－2322,
769 doi: 10.1038/srep18686, 2016.
770 Yu, B., Wang, X., Lin, C. J., Fu, X. W., Zhang, H., Shang, L. H., Feng, X. B.:
771 Characteristics and potential sources of atmospheric mercury at a subtropical
772 near-coastal site in East China, J. Geophys. Res.-Atmospheres, 120(16), 8563－
773 8574, doi:10.1002/2015JD023425, 2015.
774 Yu, B., Fu, X. W., Yin, R. S., Zhang, H., Wang, X., Lin, C. J., Wu, C. S., Zhang, Y. P.,
775 He, N. N., Fu, P. Q., Wang, Z. F., Shang, L. H., Sommar, J., Sonke, J. E.,
776 Maurice, L., Guinot, B., Feng, X. B.: Isotopic composition of atmospheric
777 mercury in China: New evidence for sources and transformation processes in air
778 and in vegetation, Environ. Sci. Technol., 50(17), 9262 － 9269, doi:
779 10.1021/acs.est.6b01782, 2016.
780 Yu, B., Yang, L., Wang, L. L., Liu, H. W., Xiao, C. L., Ling, Y., Liu, Q., Yin, Y. G., Hu,
781 L. G., Shi, J. B., Jiang, G. B.: New evidence for atmospheric mercury
782 transformations in the marine boundary layer from stable mercury isotopes,
783 Atmos. Chem. Phys., 20, 9713－9723, doi: 10.5194/acp-20-9713-2020, 2020.
784 Zambardi, T., Sonke, J. E., Toutain, J. P., Sortino, F., Shinohara, H.: Mercury
785 emissions and stable isotopic compositions at Vulcano Island (Italy), Earth
786 Planet. Sci. Lett., 277, 236－243, doi: 10.1016/j.epsl.2008.10.023, 2009.
787 Zhang, L., Wang, S. X., Wang, L., Wu, L., Duan, L., Wu, Q. R., Wang, F. Y., Yang, M.,
788 Yang, H., Hao, J. M., Liu, X.: Updated emission inventories for speciated
789 atmospheric mercury from anthropogenic sources in China, Environ. Sci.
790 Technol., 49(5), 3185－3194, doi: 10.1021/es504840m, 2015.
791 Zheng, W., Obrist, D., Weis, D., Bergquist, B. A.: Mercury isotope compositions
792 across North American forests, Global Biogeochem. Cy., 30(10), 1475－1492,
793 doi: 10.1002/2015gb005323, 2016.